First investigations on subtractive modeling with the condensed transfer functions method

Florent Dumortier, Laurent Maxit, Valentin Meyer

FIRST INVESTIGATIONS ON SUBTRACTIVE MODELING WITH THE CONDENSED TRANSFER FUNCTIONS METHOD

Florent Dumortier[1,2] **Laurent Maxit**[1] **Valentin Meyer**[2]
[1] Laboratoire Vibrations Acoustique, INSA de Lyon, France
[2] Naval Group Research, 199 avenue Pierre-Gilles de Gennes, 83190 Ollioules, France
florent.dumortier@insa-lyon.fr

ABSTRACT

Acoustic coatings are of primary importance when investigating the vibro-acoustic behavior of submerged cylindrical shells. These coatings can be applied on the entire circumference of the shell, or only on a certain stretch or a given angular domain. The latter configuration induces in the models a coupling of the shell circumferential orders, thus resulting in much heavier computation costs. To tackle this issue, it is suggested to simulate the vibroacoustic behavior of the partially coated submerged shell by using subtractive modeling. The principle of the method is to model the partially coated submerged shell, from the model of the fully coated submerged shell to which we remove a given part of the coating. In order to test its validity and its robustness to model errors, the method was at first applied to the academic case of the decoupling of Euler-Bernoulli beams. Several beam models were considered for the subtraction (analytical, FEM). The numerical results were compared to analytical calculations. Through this study, the method's sensibility to model errors was investigated and the results allow to give a first validation of the method. The results of this research will allow us extending the principle of subtractive modeling to a three-dimensional system through the study of the scattering of a plane wave by a rigid sphere.

1. INTRODUCTION

Sub-structuring methods in vibroacoustics and structural acoustics have been widely investigated over the last decades in order to overcome the frequency limitations of numerical methods. Sub-structuring methods based on impedance concepts give the possibility to couple subsystems which characteristics can be determined by different means (analytical, numerical, experimental) to assess the vibroacoustic behavior of complex structures [1].

The receptance method is a sub-structuring method based on transfer function concepts that was first introduced by Firestone as an analogy between mechanical a electrical systems [2]. It was then used by Bishop and Johnson [3] to obtain the receptances, the principal modes and the frequency equations of systems that consist in two sub-systems linked at a single or several co-ordinates. For linear problems, this method was extended to sub-systems coupled along surfaces by Ouisse et al [4], through the concept of Patch Transfer Functions (PTF). These surfaces can either be a junction between a structure and a fluid domain or a junction between two fluid domains, and are divided into patches to calculate the transfer functions. Meyer et al [5] proposed a sub-structuring approach called the Condensed Transfer Function (CTF) method, which is a generalization of the PTF method to vibro-acoustic partitioning with line or surface junctions. This method was developped in order to take into account non-axisymmetric internal structures in the study of stiffened cylindrical shells.

In this article, a reverse formulation of the receptance method (corresponding to the CTF method for point coupling) is proposed to study the decoupling of dynamic problems. The inversion of the coupling problem was first derived by Soedel and Soedel [6] to remove unwanted parts of an automotive suspension system when measuring its transfer functions. Here, the reverse receptance method is used to study the decoupling of Euler-Bernoulli beams. The objective is to derive the receptance of a beam, consisting in two beams uncoupled at a single coordinate, and for which the receptances are known (figure 1).

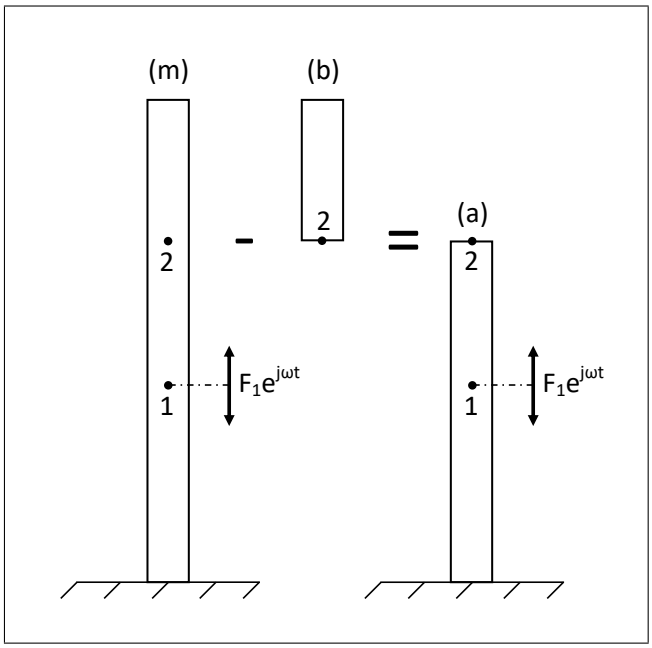

Figure 1. Decoupling of beams.

2. PRINCIPLE OF THE REVERSE RECEPTANCE METHOD

For linear systems, the receptance represents the ease of motion of the structure when subjected to a harmonic point force. Let a linear mechanical system be excited by such a force, with a given amplitude F, enabling the system to take up a steady motion of frequency ω. The point of application of the force has the displacement

$$x = Xe^{i\omega t} \tag{1}$$

As the equations of motion are linear, this may be written

$$x = \alpha F e^{i(\omega t+\phi)} \tag{2}$$

The quantity α represents the "direct receptance" at x, as the displacement is taken at the point of application of the force. If the displacement is taken at some point of the system other than the point of application of the force, then α will be defined as "cross receptance". Hence, the cross receptance corresponding to a displacement at point n caused by a force applied at point m will be

$$\alpha_{nm} = \frac{X_n}{F_m} \tag{3}$$

One has to keep in mind that α_{nm} is a complex value, taking into account the phase shift between the force and the displacement. Based on Maxwell reciprocity principle, receptances are symetric, which means that $\alpha_{nm} = \alpha_{mn}$.

Let us consider the coupling problem presented on figure 2. We want to derive the receptances μ of the beam (m) from the receptances α and β of the beams (a) and (b) (respectively). The beam (a) is excited at point 1 by a harmonic longitudinal force of amplitude F_1, and according to the Euler-Bernoulli beam theory, shear deformations are neglected. The coupling forces at point 2 also have to be taken into account when evaluating the displacements of beams (a) and (b).

Based on the superposition principle, for the coupled system, the displacements of beams (a) and (m) are given by

$$\begin{array}{l} X_1^a = X_1^m = \alpha_{11}F_1^a + \alpha_{12}F_2^a \\ X_2^a = X_2^m = \alpha_{21}F_1^a + \alpha_{22}F_2^a \end{array} \tag{4}$$

As no external force is applied on beam (b), only the coupling force at point 2 is to take into account

$$X_2^b = \beta_{22}F_2^b \tag{5}$$

For the uncoupled system, quantities α and β remain unchanged. The displacement continuity and force equilibrium between beams (a) and (b) at point 2 give the following equations

$$\left\{ \begin{array}{l} X_2^a = X_2^b \\ F_2^a + F_2^b = 0 \end{array} \right. \tag{6}$$

From system 6, we can derive the displacements of beam (m) as a function of the receptances of beams (a) and (b) and force F_1

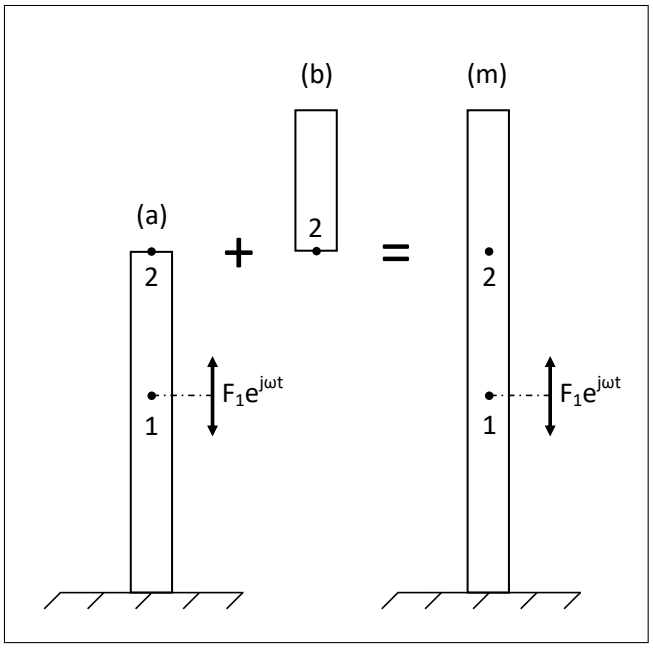

Figure 2. Coupling of beams.

$$X_1^m = \left(\alpha_{11} - \frac{\alpha_{21}^2}{\alpha_{22}+\beta_{22}}\right)F_1, \quad X_2^m = \frac{\alpha_{21}\beta_{22}}{\alpha_{22}+\beta_{22}}F_1 \tag{7}$$

The first two receptances of beam (m) directly appear in equation 7

$$\mu_{11} = \alpha_{11} - \frac{\alpha_{21}^2}{\alpha_{22}+\beta_{22}}, \quad \mu_{21} = \frac{\alpha_{21}\beta_{22}}{\alpha_{22}+\beta_{22}} \tag{8}$$

To evaluate the third receptance of beam (m), μ_{22}, the external force must be applied at coupling point 2, and the same calculations as previously must be done. The result is the following

$$\mu_{22} = \frac{\alpha_{22}\beta_{22}}{\alpha_{22}+\beta_{22}} \tag{9}$$

Now that the coupling problem has been solved, the decoupling problem can be studied (figure 1). The objective is now to derive the receptances of beam (a), knowing the receptances of beams (b) and (m).

The unknowns are now α_{11}, α_{12} and α_{22}, and they can be obtained by inverting the system of equations composed of equations 8 and 9.

$$\left\{ \begin{array}{l} \alpha_{11} = \frac{\mu_{11}(\mu_{22}-\beta_{22})-\mu_{12}^2}{\mu_{22}-\beta_{22}} \\ \alpha_{12} = -\frac{\mu_{12}\beta_{22}}{\mu_{22}-\beta_{22}} \\ \alpha_{22} = -\frac{\mu_{22}\beta_{22}}{\mu_{22}-\beta_{22}} \end{array} \right. \tag{10}$$

In the next section, these equations will be tested on beams for which receptances have be calculated with different methods (analytical, finite elements modeling).

3. NUMERICAL STUDY

3.1 Test case parameters

To illustrate the method presented above, let us consider the beams shown on figure 1 for which the mechanical characteristics and dimensions are given in the table 1.

Parameter	Notation	Value	Unit
Young modulus	E	210	GPa
Poisson coefficient	ν	0.3	-
Density	ρ	7800	kg/m^3
Structural damping coeff.	η	0.02	-
Celerity of long. waves	c_t	3220	m/s
Length of beam (a)	L_a	2	m
Length of beam (b)	L_b	0.5	m
Length of beam (m)	L_m	2.5	m
Section of the beams	S	0.05^2	m^2
Point of application of F_1	L_1	1	m

Table 1. Mechanical characteristics and beams dimensions.

As mentioned in section 2, there are different ways to compute the receptances of the beams. The first possibility is to derive them analytically, using the forced wave decomposition described by Guyader [7]. The receptances are then expressed using the wavenumber k, the Young modulus E and the geometry of the beams. The analytical receptances will serve as a reference calculation for the decoupling.

The second possibility is to create numerical models of the beams, and compute the receptances using the Finite Element Method (FEM). The beams are modeled using beam elements with the section indicated in table 1. Harmonic responses are calculated for frequencies lying between 10 Hz and around 5 000 Hz, with 500 values logarithmically spread over the domain, in order to describe properly the resonances and anti-resonances of the system. The size of the mesh is chosen to be equal to 0.1m in order to satisfy the criterion of 6 elements per wavelength (which is commonly used for the convergence of such problems), and to have a regular number of elements along the beams. With these conditions satisfied, the highest computation frequency reaches 5 367 Hz. The structural dampling coefficient is accounted for as a complex factor in the Young modulus value.

Several combinations of receptances are possible to study the decoupling of the beams (m) and (b), in order to compare the results with the analytical receptances of beam (a). At first, the analytical receptances can be used for both of the beams, in order to validate the equations of system 10. It is also possible to use for both beams the receptances calculated with the FEM method to validate the decoupling numerically. The last possibility is to use a combination of analytical and FEM receptances for the decoupling calculation. In the following sections, the results will be presented for the hybrid configuration : the receptances of beam (m) will be computed analytically, while the receptances of beam (b) will be calculated with the FEM method. This choice is justified by the final objective of the subtractive modeling, which is to model the partially coated submerged shell, from the model of the fully coated submerged shell to which we remove a given part of the coating. In this situation, the model of the fully coated submerged shell will be taken from litterature, while the removed part of the coating will be modeled by FEM.

3.2 Results

In the following sections, results for the decoupling of analytically computed (m) beam and FEM computed (b) beam will be presented and discussed. The figures will only show the direct receptance at the coupling point α_{22}, but the results for receptances α_{11} and α_{12} are somewhat similar.

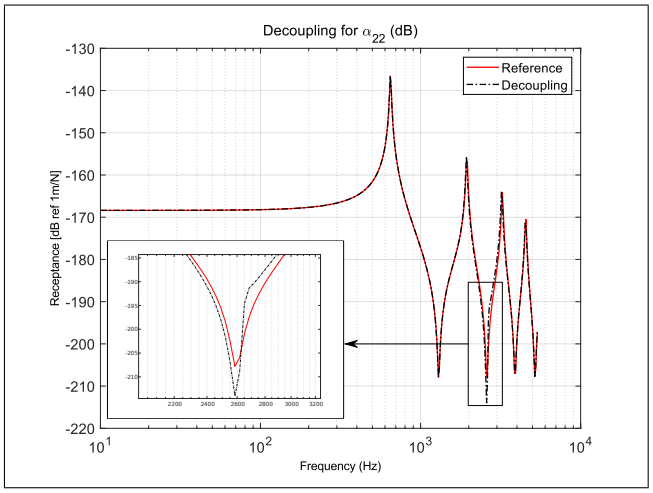

Figure 3. Receptance α_{22} obtained by decoupling.

The receptance α_{22} obtained by decoupling between beams (m) and (b) is presented on figure 3, plotted as a function of frequency. The results show a good fit between the two curves in the entire frequency range, with minor deviations around 2 600 Hz. However, it can be interesting to study the causes of these errors, in order to evaluate the method's sensibility to model errors.

3.2.1 Analysis of errors

Looking at the third equation of system 10, we have

$$\alpha_{22} = -\frac{\mu_{22}\beta_{22}}{\mu_{22} - \beta_{22}} \tag{11}$$

We can derive the small variations of α_{22} due to the small variations of β_{22} and μ_{22}. As the analytical calculation serves as a reference and the receptances of beam (m) have been calculated analytically, there are no errors on μ_{22}, therefore

$$\delta\alpha_{22} = -\frac{\mu_{22}^2}{(\mu_{22} - \beta_{22})^2}\delta\beta_{22} \tag{12}$$

Let's define, for each frequency, the coefficient γ as the ratio between β_{22} and μ_{22}, so that $\beta_{22} = \gamma\mu_{22}$. The error on α_{22} now becomes

$$\delta\alpha_{22} = -\frac{1}{(1-\gamma)^2}\delta\beta_{22} \tag{13}$$

From equation 13, we can assume that there are two main sources of errors on α_{22} : when the error on β_{22} is high (which means that the numerical error of the model are important), and when the receptances β_{22} and μ_{22} are equal or close ($\gamma = 1$). From figure 3, as the error on α_{22} is the highest around 2600 Hz, we could assume that at least one of the two conditions previously mentioned are satisfied, which would explain the encountered errors. The error on β_{22} is shown on figure 4, while the receptances β_{22} and μ_{22} are plotted together on figure 5.

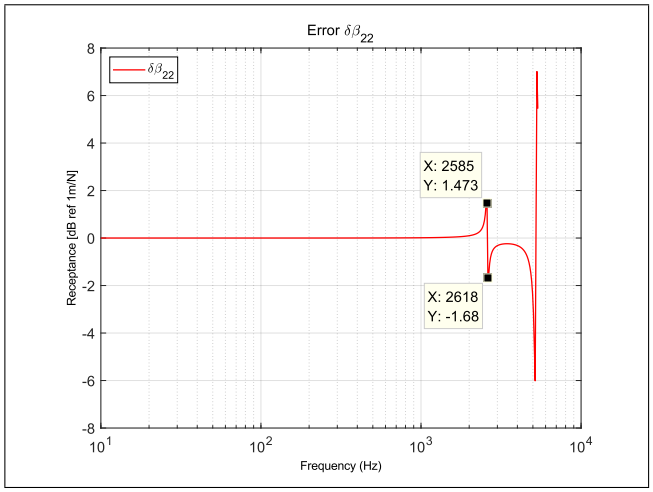

Figure 4. Error on β_{22}.

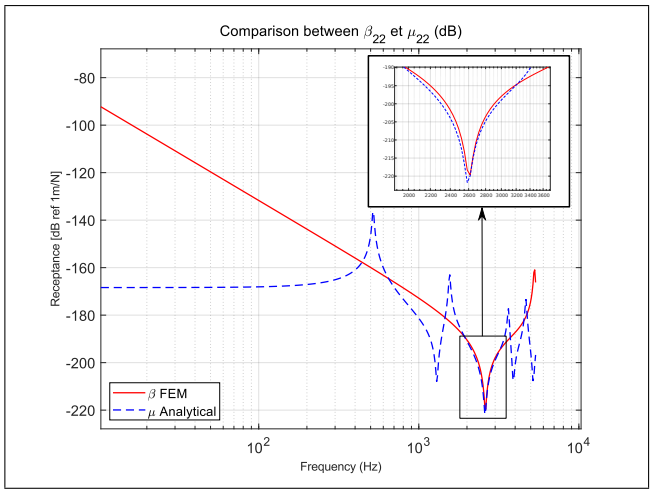

Figure 5. Comparison between β_{22} and μ_{22}.

Having a look at figures 4 and 5, at frequencies around 2 600 Hz, the two critical conditions are indeed satisfied, which explains the errors made at these frequencies. On figure 4, we notice that the errors on β_{22} are significant for the resonant frequency (around 5 300 Hz) and the anti-resonant frequency (around 2 600 Hz). At other frequencies where receptances of β_{22} and μ_{22} cross (i.e. 442 Hz), there is no signficant error made on α_{22} as the error on β_{22} is close to zero. Hence, limiting numerical errors on β_{22} by applying a finer mesh on the FEM model will allow avoiding errors on α_{22}. As the beam is relatively small and there aren't many elements on the beam's length, refining the mesh won't affect much the calculation time. However, on more complex structures, one has to keep in mind that this solution may severely increase the computation costs.

Alternatively, the errors will be small if β_{22} and μ_{22} will be significantly different. Two cases have been studied in this work and will be developped in the following sections.

3.2.2 Influence of the length of beam (b)

One could assume that the length of beam (b) plays a key role on the error made on the receptances of beam (a) when the decoupling is done. Indeed, with the length of beam (m) unchanged, we could state that the longer the beam (b) to be removed, the bigger its influence on the receptances of beam (m), and then the bigger the error on the receptances of beam (a). Having a look at figure 5, we can see that the receptance β_{22} follows the shape of μ_{22} on the anti-resonance around 2 600 Hz.

Receptances β_{22} and μ_{22} are once again compared for two differents lengths of beam (b) (L_b=0.3 m and L_b=1.2 m) in order to validate the previous statement (figure 6). We can see that, indeed, when beam (b) is longer, its receptance β_{22} has several anti-resonances in common with μ_{22}, which will probably lead to more errors on α_{22}, as absolute errors on β_{22} are high at these frequencies.

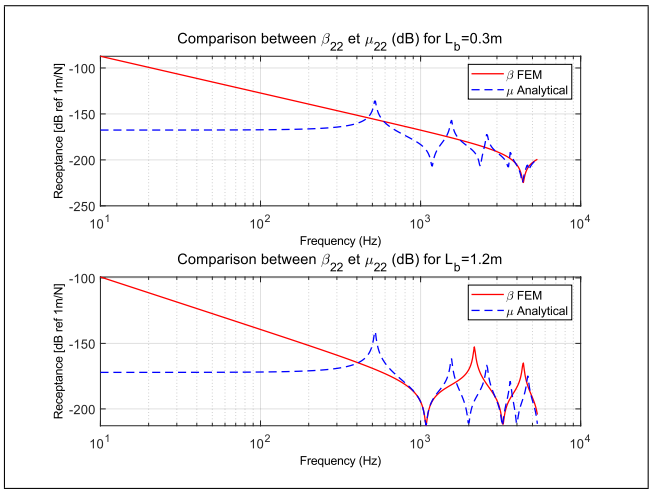

Figure 6. Comparison of β_{22} and μ_{22} for different lengths of beam (b)

Figure 7 shows that there are indeed more critical frequency domains where the error on α_{22} is high when the length of the beam to beam removed is more important. We can conclude that the errors made on α_{22} are directly linked to the anti-resonances of β_{22}.

To validate the influence of the length of beam (b), the evolution of the relative error between the receptances α computed analytically and the receptances α computed by decoupling between the beams (m) (analytically computed) and (b) (computed with FEM modeling), as a function of the length of beam (b), is presented on figure 8. The

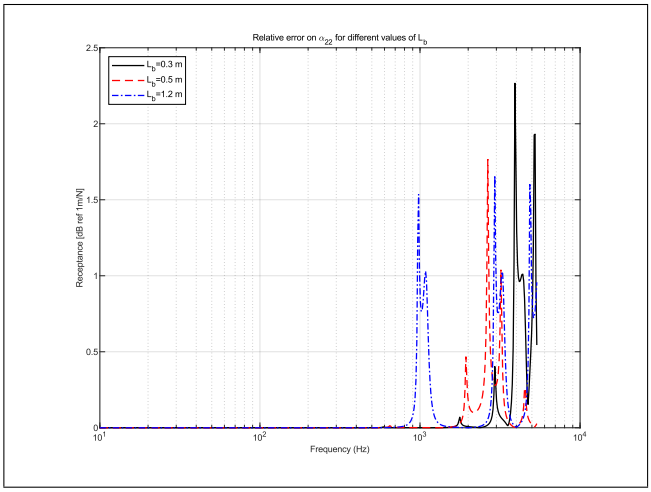

Figure 7. Relative error on α_{22} for several lengths of beam (b)

values displayed on figure 8 are mean values computed over the whole frequency range. The length of beam (b) was varied from 0.1 m to 1.4 m with increments of 0.1 m. The global behavior of these curves confirms the asumption made previously about the impact of the size of the decoupled beam, as the error increases when the size of the beam (b) is augmented. Another observation from figure 8 is that the receptance α_{11} is more sensitive to errors than receptances α_{12} and α_{22}, which may be explained by the fact that the expression of α_{11} (equation 10) depends on more parameters than α_{12} and α_{22}

$$\delta\alpha_{11} = -\frac{1}{(1-\gamma)^2} \cdot \left(\frac{\mu_{12}}{\mu_{22}}\right)^2 \delta\beta_{22} \qquad (14)$$

The factor $(\mu_{12}/\mu_{22})^2$ may explain the amplification of the error made on α_{11} compared to α_{22} as observed in figure 8.

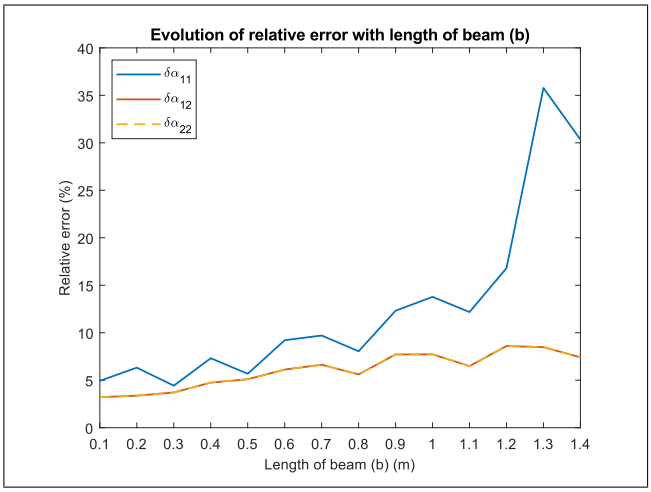

Figure 8. Influence of length of beam (b).

To put this analysis into the global perspective of this study, we could assume that the principle of subtractive modeling applied to the partially coated cylindrical shell would be less sensitive to model errors if the part of the coating that is to be removed remains small compared to the size of the shell.

3.2.3 Influence of structural damping

One studies now the influence of the beam damping on the decoupling results. Indeed, increasing the structural damping could have beneficial effects on the stability of the method, since it would reduce the amplitude of the resonances and anti-resonances, thus leading to less frequency ranges that would be impacted by the crossing of receptances. Furthermore, regarding the final application of the method, the coating applied on cylindrical shells is made of viscoelastic materials, which have a much higher structural damping coefficient than metal. Hence, the calculations made previously were reiterated with a structural damping coefficient of 0.2 (against 0.02 previously). The geometrical parameters of the beams are the ones defined in table 1.

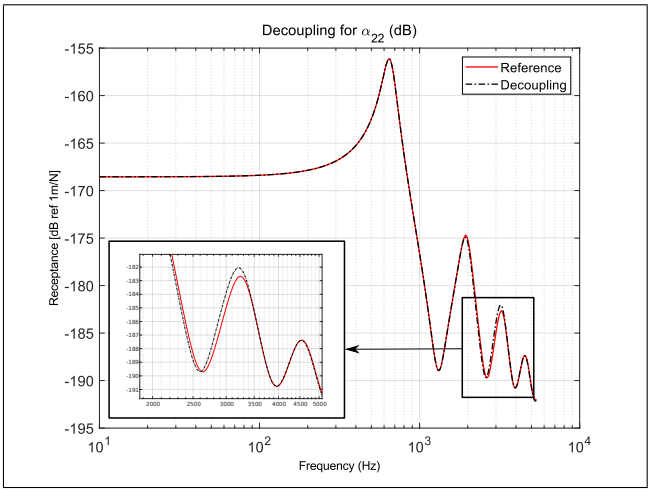

Figure 9. Influence of structural damping.

The receptance α_{22} obtained with a higher structural damping coefficient is displayed on figure 9 and shows that the reference curve and the decoupling curve fit almost perfectly. There are still minor errors around 3 000 Hz, which are smaller than the ones we saw on figure 3 (the maximum error is 7 times smaller, and the relative error is twice smaller for a mesh size of 0.1 m). It is still interesting to study the influence of errors as in section 3.2. The two main sources of errors (model error on β_{22} and crossings between β_{22} and μ_{22}) are presented on figure 10.

With the same geometrical and mechanical parameters (except the structural damping coefficient) and the same mesh size, it is interesting to note that the model errors on β_{22} have been reduced by a factor 10. Also, in the frequency range where the two receptances have the same shape, the values of the receptances are not as close to each other as they are on figure 5. This means that even when the two critical conditions are satisfied, the error made on α_{22} is limited, as can be seen on figure 11. The amplitude of the relative error has a maximum of 0.16, which is about ten times lower than the relative error computed

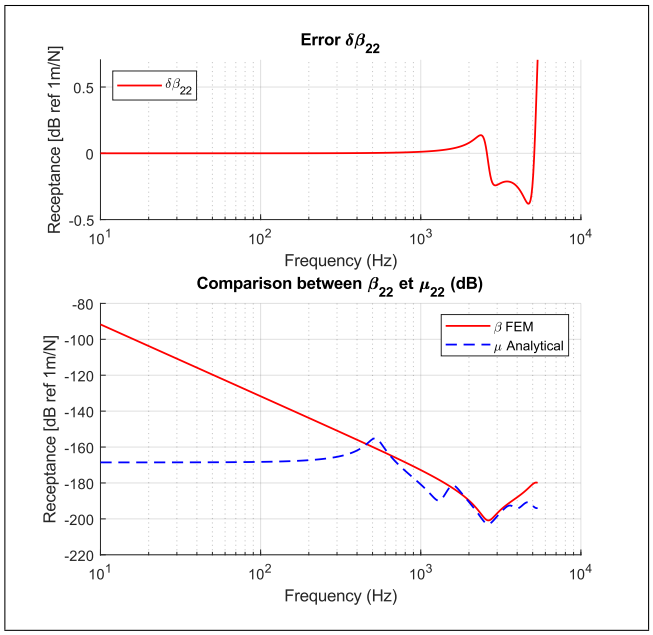

Figure 10. Sources of errors with higher structural damping.

with a structural damping coefficient of 0.02, for the same dimensions of the beams.

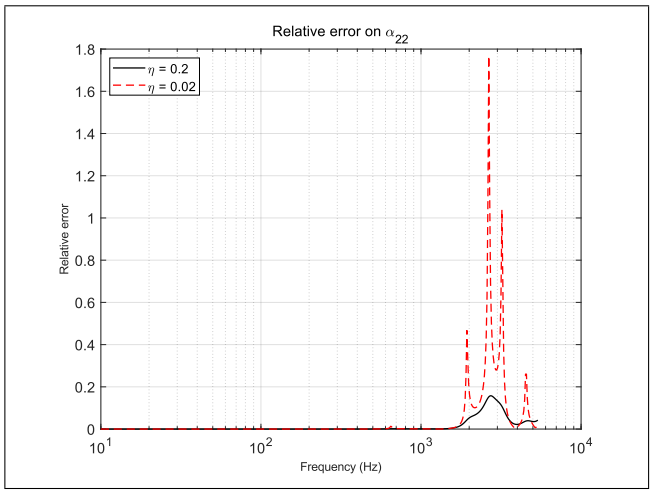

Figure 11. Relative error on α_{22} with a higher structural damping coefficient.

The conclusion drawn in this section is thus encouraging in view of applying subtractive modeling with viscoelastic materials, for which the structural damping coefficient is much higher than for steel.

4. CONCLUSION

The concept of subtractive modeling has been applied, as a first step, to the decoupling of beams via the reverse receptance method. The receptances of a beam (a) have been calculated by removing a part (b) of the beam (for which the receptances have been computed using a FEM model) from a longer beam (m) (for which the receptances have been computed analytically). These receptances have been compared to the receptances of beam (a) computed analytically. The results of this first study show a good convergence of the method, with some main sources of errors that have been identified. Two conclusions can be drawn from the results :

- the lower the size of the uncoupled structure will be, the lower the errors in the model and thus in the decoupling.
- the higher the structural damping coefficient will be, the lower the errors as the amplitudes of the resonances are reduced.

In the perspective of applying the principle of subtractive modeling to the partially coated cylindrical shell, and in order to study further the method's sensibility to model errors, the principle of subtractive modeling will be extended on a three-dimensionnal study : the scattering of a plane wave by a rigid sphere, using the CTF method [5]. Analytical and numerical results showing good agreement for this test case will soon be released.

5. REFERENCES

[1] G.J. O'Hara. Mechanical impedance and mobility concepts. *Journal of the Acoustical Society of America*, 41:1180–1184, 1967.

[2] F.A. Firestone. The mobility method of computing the vibration of linear mechanical and acoustical systems: mechanical-electrical analogies. *Journal of Applied Physics*, 9(6):373–387, 1938.

[3] R.E.D. Bishop and D.C. Johnson. *The Mechanics of Vibration*. Cambridge University Press, 1979.

[4] M. Ouisse, L. Maxit, C. Cacciolati and J.-L. Guyader. Patch transfer functions as a tool to couple linear acoustic problems. *Journal of Vibration and Acoustics*, 127:458–466, 2005.

[5] V. Meyer, L. Maxit, J.-L. Guyader, T. Leissing and C. Audoly. A condensed transfer function method as a tool for solving vibroacoustic problems. *Proc. of the Institution of Mechanical Engineers, Part C: Journal of Mechanical Engineering Science* , SAGE Publication, 2015.

[6] D.T. Soedel and W. Soedel. Synthetising reduced systems by complex receptances. *Journal of Sound and Vibration*, 179(5):855–867, 1994.

[7] J.-L. Guyader. *Vibrations des milieux continus*. Hermes Sciences, 2002.